doi: 10.13241/j.cnki.pmb.2019.05.022

弹性成像定量分析联合硬环征在甲状腺良恶性结节鉴别诊断中的应用价值分析 *

牛 艳[1,2] 周 琦[1△] 李 娜[2] 钟 娜[2] 吴 琼[2] 刘 慧[2] 刘慧平[3]

（1 西安交通大学第二附属医院超声研究室 陕西 西安 710004；2 榆林市星元(第四)医院超声科 陕西 榆林 719000；
3 榆林市北方医院超声科 陕西 榆林 719000）

摘要 目的：探究弹性定量分析联合硬环征在甲状腺良恶性结节鉴别诊断中的应用价值。**方法：**回顾性分析 2018 年 1 月至 2018 年 9 月于我院行手术或穿刺活检病理证实的 121 例甲状腺结节患者临床资料，所有患者均行弹性成像定量分析以及剪切波弹性成像(SWE)分析，计算弹性成像定量分析、SWE 分析以及联合检测，以病理检查结果为金标准(良性 78 个，恶性 43 个)，对甲状腺良恶性结节诊断的敏感性、特异度、准确性、阳性预测值以及阴性预测值，分别绘制弹性成像定量分析、SWE 以及联合检测的受试者工作特征(ROC)曲线，并比较 ROC 曲线下面积。**结果：**(1)弹性定量分析诊断良性结节 87 个，恶性 34 个，敏感性 73.08%，特异度 30.23%，阳性预测值 65.51%，阴性预测值 38.24%；(2)SWE 分析良性结节 76 个，恶性结节 45 个，敏感性 64.10%，特异度 39.53%，阳性预测值 65.79%，阴性预测值 37.78%；(3)联合检测良性结节 73 个，恶性结节 48 个，敏感性 89.74%，特异度 93.02%，阳性预测值 95.89%，阴性预测值 83.33%；(4)联合检测敏感性、特异度、阳性预测值及阴性预测值均高于单独检测(P <0.05)；(5)弹性成像定量分析、SWE 及联合检测 ROC 曲线下面积分别为 0.843、0.819、0.940，联合检测准确率高于单一检测(P<0.05)；SWE 分析甲状腺良恶性结节的弹性模量值 Emean、Emin、Emax、Esd、Emean-p 及 Emean-m 均显著大于恶性结节(P <0.05)。**结论：**弹性成像定量分析联合硬环征检测能够显著提高对甲状腺结节良恶性病变的诊断敏感性及特异度，具有较高的临床应用价值。

关键词：弹性成像定量分析；硬环征；甲状腺结节；良恶性病变

中图分类号：R736.1 **文献标识码：**A **文章编号：**1673-6273(2019)05-894-05

Analysis of the Application value of Elastography Quantitative Analysis Combined with Hard Ring Sign for the Differential Diagnosis of Benign and Malignant Thyroid Nodules*

NIU Yan[1,2], ZHOU Qi[1△], LI Na[2], ZHONG Na[2], WU Qiong[2], LIU Hui[2], LIU Hui-ping[3]

*(1 Ultrasound laboratory, The Second Affiliated Hospital of Xi'an Jiao Tong University, Xi'an, Shaanxi, 710004, China;
2 Ultrasonography Department, The First Affiliated Hospital of Xi'an Jiao Tong University, Xi'an, Shaanxi, 710004, China;
3 Ultrasonography Department, Xingyuan (fourth) Hospital of Yulin, Yulin, Shaanxi, 719000, China)*

ABSTRACT Objective: To explore the diagnostic value of elastic quantitative analysis combined with hard ring sign for differentiating benign and malignant thyroid nodules. **Methods:** The clinical data of 121 cases of patients with thyroid nodules confirmed by operation or biopsy in our hospital from January 2018 to September 2018 were retrospectively analyzed. All the patients underwent elastography quantitative analysis and shear wave elastography (SWE) analysis. Quantitative analysis of elastography, SWE analysis and combined detection were performed. The results were golden standard (78 benign and 43 malignant), sensitivity, specificity, accuracy, positive predictive value and negative predictive value for the diagnosis of benign and malignant thyroid nodules. Quantitative analysis of elastography, SWE and ROC curves were drawn respectively, and the areas under ROC curves were compared. **Results:** (1) Elastic quantitative analysis of 87 benign nodules, 34 malignant, the sensitivity was 73.08%, the specificity was 30.23%, the positive predictive value was 65.51%, the negative predictive value was 38.24%; (2) SWE analysis of 76 benign nodules, 45 malignant nodules, the sensitivity was 64.10%, the specificity was 39.53%, the positive predictive value was 65.79%, the negative predictive value was 37.78%; (3) 73 benign nodules, 48 malignant nodules, the sensitivity was 89.74%, the specificity was 93.02%, the positive predictive value was 95.89%, the negative predictive value was 83.33%; (4) The sensitivity, specificity, positive predictive value and negative predictive value of combined detection were higher than those of single detection (P<0.05); (5) Quantitative analysis of elastography. The area under ROC curve was 0.843, 0.819 and

* 基金项目：陕西省社会发展科技攻关项目(2015SF057)

作者简介：牛艳(1982-)，女，本科，主治医师，研究方向：浅表器官，电话：15686769998，E-mail：niuyan198227@163.com

△通讯作者：周琦(1966-)，女，博士，主任医师，研究方向：超声甲状腺、乳腺等浅表器官及胎儿超声的诊断及鉴别诊断及超声造影等新技术的应用，电话：13909232905，E-mail：niuyan198227@163.com

(收稿日期：2018-11-08 接受日期：2018-11-30)

0.940, respectively. The accuracy of combined detection was higher than that of single method (P<0.05). SWE analysis of the modulus of elasticity of benign and malignant thyroid nodules Emean, Emin, Emax, Esd, Emean-p and Emean-m were significantly larger than the malignant nodules (P<0.05). **Conclusion:** Quantitative analysis of elastography combined with hard ring sign detection can significantly improve the sensitivity and specificity in the diagnosis of benign and malignant thyroid nodules, and it has high clinical value.

Key words: Elastography quantitative analysis; Hard ring sign; Thyroid nodule; Benign and malignant lesions

Chinese Library Classification(CLC): R736.1 Document code: A

Article ID: 1673-6273(2019)05-894-05

前言

甲状腺是位于颈部甲状软骨下方、气管两旁的重要内分泌器官,具有控制能量使用速度、制造蛋白质、调节机体对其他荷尔蒙敏感性的作用,甲状腺能够通过分泌甲状腺素来对机体的生理活动进行调节,是人体最大的内分泌腺[1,2]。甲状腺结节是指在甲状腺内的肿块,能够随个体的吞咽动作而上下移动,是临床上常见的疾病,根据其病理类型可将其分为退行性病变、炎症、自身免疫等。甲状腺结节可发于任何年龄,正常人群中检出率约为 19%-76%[3,4]。甲状腺结节有机率发展为甲状腺癌,约占全身恶性肿瘤的 1%[5]。早期甲状腺癌临床症状并不明显,因而存在漏诊现象,晚期甲状腺癌治疗难度较大,患者生活质量将会严重降低。早期检查及干预是提高甲状腺癌患者预后的重要手段[6,7]。

现阶段甲状腺结节良恶性病变的诊断方式主要为影像学检查,包括超声、CT、磁共振等,这些方式具有费用低、无创、无辐射等优点,但各类方式在鉴别甲状腺结节良恶性病变中的价值不一[8,9]。近年来发展起来的实时剪切波弹性成像(SWE)技术为临床提供了一种量化分析甲状腺结节硬度的有效手段。本研究主要探讨了弹性定量分析联合硬环征在甲状腺良恶性结节鉴别中的诊断应用价值,报道如下。

1 资料与方法

1.1 一般资料

回顾性分析 2018 年 1 月至 2018 年月 6 于我院行手术或穿刺活检病理证实的 121 例甲状腺结节患者临床资料,患者中男性 50 例,女性 71 例,年龄 26-67 岁,平均年龄(43.06± 2.18)岁,结节最大直径 7-23 mm,平均直径为(13.26± 2.17)mm。

纳入标准[10]:(1)经检查确诊存在甲状腺结节;(2)甲状腺功能正常;(3)具有外科手术可触碰或不可触碰的结节;(4)病历资料齐全;(5)调研经医院伦理学会批准实施;(6)患者及其家属知情同意。

排除标准:(1)年龄≤ 18 周岁;(2)合并精神疾患者;(3)妊娠或哺乳期女性;(4)合并其他恶性肿瘤者;(5)合并严重肝肾功能障碍者。

1.2 方法

所有入组患者均首先实施弹性成像定量分析,患者取仰卧位,头后仰,暴露颈部,使用西门子 ACUCON+S2000 型彩色超声仪在患者颈前区从不同切面(横切、纵切、斜切)扫描甲状腺,确定甲状腺结节部位后切换为弹性成像系统,获取甲状腺结节部位的弹性定量分析[11,12]。而后选用最佳的切面,对所有患者实施 SWE 检测,使用仪器为迈瑞 Resona 7 超声诊断仪,预设弹性模量值测量范围为 0～100 kPa。患者取仰卧位,取样框稍大于结节部位,探头轻触皮肤,注意不要实施压力,嘱患者屏气,应用仪器分析 Q-BOXTM 组织弹性定量分析系统测量取样框内各项弹性模量值,然后选取病变组织中最硬处区域与正常甲状腺组织及前方肌肉,测量弹性模量比值(Emean-p 和 Emean-m)(本试验选取取样框的直径为 2 mm)。

病灶由经验丰富的超声医师重复上述操作 3 次,取平均值为最终测量值。

1.3 评测标准

1.3.1 弹性成像定量分析标准 结节全部为均匀蓝色(质硬)为 4 分;结节大部分为蓝色,仅有些许绿色为 3 分;结节大部位为绿色,但存在些许蓝色区域为 2 分;结节整体显示为均匀绿色(质软)为 1 分。1-2 分评定为良性,3-4 分为恶性[13,14]。

1.3.2 硬环征标准 SWE 图像分析参照如下标准:红色代表硬组织,蓝色代表软组织,绿色代表中间硬度组织,定义硬环征为与正常甲状腺组织相比,结节周边硬度明显增加(颜色呈现黄色或红色),呈现环状变化[15,16]。

1.4 观察指标

(1)患者的病理学结果;(2)弹性成像定量分析、硬环征分析及两种方法联合检测检出率及灵敏度、特异度、准确度、阳性预测值及阴性预测值对比。灵敏度 =(真阳性)/(真阳性 + 真阴性);特异度 = 假阴性 /(假阳性 + 假阴性);准确度 =(真阳性 + 假阴性)/ 总数;阳性预测值 = 真阳性 /(真阳性 + 假阴性);阴性预测值 = 假阴性 /(真阴性 + 假阴性);(3)三种方式 ROC 曲线分析;(4)SWE 分析甲状腺良恶性结节的弹性模量值比较。

1.5 统计学方法

使用 SPSS16.0 对数据进行统计学分析,计数资料组件比较采用卡方检验,计量资料组间比较采用 t 检验,以 P<0.05 为差异有统计学意义。

2 结果

2.1 患者的病理学检查结果

入院后,病理检查甲状腺结节呈良性的有 78 个,恶性结节有 43 个,以此作为检测的金指标。

2.2 弹性成像定量分析、SWE 分析结果及两者联合良恶性检出结果

弹性定量分析诊断良性结节 87 个,恶性 34 个,敏感性 73.08%,特异度 30.23%,阳性预测值 65.51%,阴性预测值 38.24%。SWE 分析良性结节 76 个,恶性结节 45 个,敏感性 64.10%,特异度 39.53%,阳性预测值 65.79%,阴性预测值 37.78%。联合检测,发现良性结节 73 个,恶性结节 48 个,敏感性 89.74%,特异度 93.02%,阳性预测值 95.89%,阴性预测值 83.33%。具体数据如表 1 所示:

表 1 弹性成像定量分析、SWE 分析结果及两者联合良恶性检出结果

Table 1 Quantitative analysis of elastic imaging, SWE analysis and the combination for the benign and malignant thyroid nodules

Pathologic resultn	n	Quantitative analysis of elastic imaging		SWE analysis		Two combined	
		Benign	Malignant	Benign	Malignant	Benign	Malignant
Benign thyroid nodules	78	57	21	50	28	70	8
Malignant thyroid nodules	43	30	13	26	17	3	40
Total	121	87	34	76	45	73	48

2.3 3 种检测方式敏感性、特异度、阳性预测值及阴性预测值的比较

经对比发现，联合检测敏感性、特异度、阳性预测值及阴性预测值均高于两项单独检测(P<0.05)，而两者单独检测敏感性、特异度、阳性预测值及阴性预测值比较无统计学差异(P>0.05)，具体数据如表 2 所示。

表 2 3 种不同检测方式检测结果对比(%)

Table 2 Comparison of the results of three different detection methods (%)

Group	Sensitivity	Specificity	Positive predictive value	Negative predictive value
Quantitative analysis of elastic imaging	73.08	30.23	65.51	38.24
SWE analysis	64.10	39.53	65.79	37.78
Two combined	89.74*	93.02*	95.89*	83.33*

Note: compared with elastic ultrasound and hard ring sign, *P<0.05.

2.4 三种检测方式的 ROC 曲线分析

经分析发现，弹性成像定量分析、SWE 及联合检测 ROC 曲线下面积分别为 0.843、0.819、0.940，联合检测准确率高于单一方法(Z=1.71、2.36，P<0.05)。

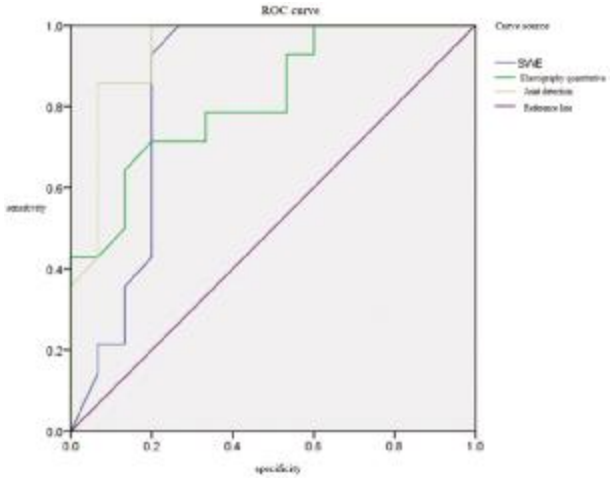

2.5 SWE 分析甲状腺良恶性结节的弹性模量值比较

SWE 分析甲状腺良恶性结节的弹性模量值均显著大于恶性结节(P <0.05)，具体数据如表 3 所示：

3 讨论

甲状腺结节是甲状腺最常见病变类型之一，且近些年该病的检出率呈现逐年递增趋势，甲状腺结节在特定因素的诱导下，有发展为甲状腺癌的机率，会对患者生命健康造成严重威胁。早期的检测及干预是提高甲状腺癌的重要手段[17,18]。现阶段甲状腺结节病变的主要检测手段包括血清学检查、核素扫描、穿刺细胞活检、颈部 X 线、甲状腺功能测定等，其中实验室指标的检测特异性较低，容易造成误诊，而活检的方式痛苦较大，患者难以接受[19,20]。超声具有无创、迅速、准确等优点，在甲状腺结节的发现、筛查、诊断中具有重要作用。研究显示接受超声检测的人群中约有 40%-50%存在甲状腺结节，其中又有约 5%会发展为甲状腺癌[21,22]，提示超声在甲状腺癌的前期检测中具有重要的应用意义，通过对甲状腺结节良恶性病变的鉴别能够为后期治疗方案的确定奠定良好的基础。

弹性成像定量分析是一种新型的超声诊断技术，临床研究显示机体组织的弹性依赖于其分子与微观结构，而组织的硬度与其病变程度及病理密切相关[23]。弹性成像定量分析能够通过对组织硬度的检测以及组织在收到外力压迫后发生变形的程度分辨病变类型，弥补了常规超声的不足，能够更加生动的显示、定位病变[24,25]。SWE 分析属于新的弹性检测方法，是振动性

表 3 SWE 分析甲状腺良恶性结节的弹性模量值比较($\bar{x}\pm s$)

Table 3 Comparison of the modulus of elasticity in benign and malignant thyroid nodules by SWE($\bar{x}\pm s$)

SWE analysis	n	Emean(kPa)	Emin(kPa)	Emax(kPa)	Esd(kPa)	Emean-p	Emean-m
Benign thyroid nodules	76	22.31± 6.22	12.42± 4.23	35.24± 10.06	6.15± 2.68	1.73± 0.68	1.69± 0.57
Malignant thyroid nodules	45	39.53± 13.54*	17.35± 8.65*	73.47± 25.82*	13.42± 4.12*	3.97± 1.76*	3.68± 2.16*

Note: compared with Benign thyroid nodules, *P<0.05.

弹性成像技术，能通过定量分析系统测量组织的弹性模量值，具有客观及重复性好的优点，避免了操作者主观性的缺陷，提高了早期甲状腺癌的诊断准确率。有些学者[26]的研究显示恶性病变与良性病变甲状腺结节患者对比可见其应变均值、蓝色区域面积、杂乱度存在明显差异，提示超声应变弹性成像量化指标能够用于甲状腺良恶性病变的区分中。硬环征属于超声检测结果中的一种，陈小爽灯的研究显示乳腺恶性病变患者会出现明显的硬环征，病变部位呈现“黑洞”样改变，提示硬环征可以作为鉴别乳腺良恶性病变的一项重要指标[27,28]。目前的研究显示甲状腺结节的弹性模量值 Emean、Emin、Emax、Esd、Emean-p 及 Emean-m 育结节的良恶性相关，可能与甲状腺良恶性的鉴别有关[29]。

本研究以病理学检查结果为金标准，发现弹性定量分析及硬环征在鉴别甲状腺良恶性病变中均具有较高的敏感性、特异度、阳性预测值及阴性预测值，而联合检测不仅具有比单独检测更高的敏感性、特异度、阳性预测值及阴性预测值，还具有更高的 ROC 曲线下面积。以上结果表明超声检查能够区分实性或囊性甲状腺结节，同时能够对结节部位各指标进行判断，帮助分辨良恶性病变，但多种方式联合的方式切实能够提高检测的准确性。弹性成像定量分析能够通过对组织软硬程度的检测来分辨结节的病变类型，因恶性病变组织边界不清晰、形态不规则，且癌变组织由于含有丰富的薄壁血管，相比于正常甲状腺组织，其硬度会有所下降，因而通过超声检测能够较为准确的分辨病变类型[30,31]。而硬环征属于结节病变的常见形态，盖因肿瘤中含有丰富的血管，恶性肿瘤一般位于其边缘部位，便于向四周及边缘地带侵袭，因而肿瘤会对周围组织施加不同大小的拉力，引发血管扭曲、扩张，造成病变周围弹性模量值相对较高，而形成硬环征，因而通过对该特征的鉴别也有助于对甲状腺结节病变类型的分辨[32,33]。同时，SWE 分析甲状腺良恶性结节的弹性模量值均显著大于恶性结节，说明 Emean、Emin、Emax、Esd、Emean-p 及 Emean-m 可以做为判断甲状腺结节良恶性的诊断标准，特别是 Emax。原因可能与其组织学依据相关，恶性病灶间质内常见钙化沙砾体，病灶细胞纤维及血管较多，质地较硬，弹性模量值较高。

总之，弹性成像定量分析联合硬环征检测能够显著提高对甲状腺结节良恶性病变的诊断敏感性及特异度，具有较高的临床应用价值。

参考文献(References)

[1] Yoon J H, Han K, Kim E K, et al. Diagnosis and Management of Small Thyroid Nodules: A Comparative Study with Six Guidelines for Thyroid Nodules[J]. Radiology, 2017, 283(2): 560-569

[2] Morris M A, Ring C M, Managuli R, et al. Feature analysis of ultrasound elastography image for quantitative assessment of cutaneous carcinoma [J]. Skin Research & Technology, 2017, 24 (3 Suppl): 242-247

[3] Ma H, An Z, Xia P, et al. Semi-quantitative Analysis of EBUS Elastography as a Feasible Approach in Diagnosing Mediastinal and Hilar Lymph Nodes of Lung Cancer Patients[J]. Scientific Reports, 2018, 8 (1): 3571-3586

[4] Shih C C, Qian X, Ma T, et al. Quantitative assessment of thin-layer tissue viscoelastic properties using ultrasonic micro-elastography with Lamb wave model [J]. IEEE Transactions on Medical Imaging, 2018, 37(8): 1887-1898

[5] Arani A, Arunachalam S P, Chang I C, et al. Cardiac MR elastography for quantitative assessment of elevated myocardial stiffness in cardiac amyloidosis[J]. Journal of Magnetic Resonance Imaging, 2017, 46(5): 1361-1367

[6] Sun Y, Ma C, Liang X, et al. Reproducibility analysis on shear wave elastography (swe)-based quantitative assessment for skin elasticity [J]. Medicine, 2017, 96(19): e6902

[7] Chiba M, Imazu H, Kato M, et al. Novel quantitative analysis of the S100P protein combined with endoscopic ultrasound-guided fine needle aspiration cytology in the diagnosis of pancreatic adenocarcinoma [J]. Oncology Reports, 2017, 37(4): 1943-1952

[8] Krepkin K, Bruno M, José G. Raya, et al. Quantitative assessment of the supraspinatus tendon on MRI using T2/T2* mapping and shear-wave ultrasound elastography: a pilot study[J]. Skeletal Radiology, 2017, 46(2): 191-199

[9] Lee S , Chung J, Choi H Y , et al. Evaluation of Screening US-detected Breast Masses by Combined Use of Elastography and Color Doppler US with B-Mode US in Women with Dense Breasts: A Multicenter Prospective Study[J]. Radiology, 2017, 285(2): 660-669

[10] Xiao X, Jiang Q, Wu H, et al. Diagnosis of sub-centimetre breast lesions: combining BI-RADS-US with strain elastography and contrast-enhanced ultrasound-a preliminary study in China [J]. European Radiology, 2016, 27(6):2443-2450

[11] Vuppalanchi R, Siddiqui M S, Natta M L V, et al. Performance Characteristics of Vibration-Controlled Transient Elastography for Evaluation of Non-Alcoholic Fatty Liver Disease [J]. Hepatology, 2018, 67 (1): 134-144

[12] Lee S H, Chang J M, Cho N, et al. Abstract P5-02-02: Combined use of elastography and color doppler ultrasound for the evaluation of breast masses detected at screening ultrasound in women with dense breasts[J]. Cancer Research, 2017, 77(4): P5-02-02-P5-02-02

[13] Ducancelle A, Leroy V, Vergniol J, et al. A Single Test Combining Blood Markers and Elastography is More Accurate Than Other Fibrosis Tests in the Main Causes of Chronic Liver Diseases [J]. Journal of Clinical Gastroenterology, 2017, 51(7): 639-649

[14] Eddowes P J, Mcdonald N, Davies N, et al. Utility and cost evaluation of multiparametric magnetic resonance imaging for the assessment of non-alcoholic fatty liver disease[J]. Alimentary Pharmacology & Therapeutics, 2018, 47(5): 631-644

[15] Maira D, Cassinerio E, Marcon A, et al. Progression of liver fibrosis can be controlled by adequate chelation in transfusion-dependent thalassemia (TDT)[J]. Annals of Hematology, 2017, 96(11): 1931-1936

[16] Zhang F, Zhao X, Han R, et al. Comparison of Acoustic Radiation Force Impulse Imaging and Strain Elastography in Differentiating Malignant From Benign Thyroid Nodules[J]. Journal of Ultrasound in Medicine, 2017, 36(12): 2533-2543

[17] Chen J, Gao J, Sun G. Quantitative analysis combined with chromatographic fingerprint and antioxidant activities for the comprehensive evaluation of Compound Danshen Tablets [J]. Journal of Separation Science, 2017, 40(6): 1244-1253

[18] Ueda J, Yoshimura H, Shimizu K, et al. Combined visual and semi-quantitative assessment of 123I-FP-CIT SPECT for the diagnosis of dopaminergic neurodegenerative diseases [J]. Neurological Sciences, 2017, 38(7): 1187-1191

[19] Sun Y, Ma C, Liang X, et al. Reproducibility analysis on shear wave elastography (swe)-based quantitative assessment for skin elasticity [J]. Medicine, 2017, 96(19): e6902

[20] Rago T, Scutari M, Loiacono V, et al. Low elasticity of thyroid nodules at ultrasound elastography is correlated with malignancy, degree of fibrosis and high expression of galectin-3 and fibronectin-1 [J]. Thyroid, 2017, 27(1): 103-110

[21] Yamamoto Y, Yamaguchi S, Sasho T, et al. Quantitative US Elastography Can Be Used to Quantify Mechanical and Histologic Tendon Healing in a Rabbit Model of Achilles Tendon Transection [J]. Radiology, 2017, 283(2): 408-417

[22] Hasanali J , Vujaskovic G, Malobabic S. Erratum: Quantitative analysis of the trigeminal ganglion neurons in the human, monkey and baboon (European Journal of Anatomy (1999) 3: 3(115-120))[J]. Journal of Cardiovascular Electrophysiology, 2017, 24(5): 503-509

[23] Kim M H, Yun C, Chalisserry E P, et al. Quantitative analysis of the role of nanohydroxyapatite (nHA) on 3D-printed PCL/nHA composite scaffolds[J]. Materials Letters, 2018, 220(56): 112-115

[24] Arani A, Arunachalam S P, Chang I C, et al. Cardiac MR elastography for quantitative assessment of elevated myocardial stiffness in cardiac amyloidosis[J]. Journal of Magnetic Resonance Imaging, 2017, 46(5): 1361-1367

[25] Lee K S, Martin J, Thelen D. Science to Practice: Quantitative US Elastography Can Be Used to Quantify Mechanical and Histologic Tendon Healing in a Rabbit Model of Achilles Tendon Transection [J]. Radiology, 2017, 283(2): 311-313

[26] Park S Y, Choi J S, Han B K, et al. Shear wave elastography in the diagnosis of breast non-mass lesions: factors associated with false negative and false positive results [J]. European Radiology, 2017, 27(9): 3788-3798

[27] Ara S R, Bashar S K, Alam F , et al. EMD-DWT Based Transform Domain Feature Reduction Approach for Quantitative Multi-class Classification of Breast Tumors[J]. Ultrasonics, 2017, 80(33): 22-33

[28] Pass B, Jafari M, Rowbotham E, et al. Do quantitative and qualitative shear wave elastography have a role in evaluating musculoskeletal soft tissue masses?[J]. European Radiology, 2017, 27(2): 723-731

[29] Krepkin K, Bruno M, José G. Raya, et al. Quantitative assessment of the supraspinatus tendon on MRI using T2/T2* mapping and shear-wave ultrasound elastography: a pilot study [J]. Skeletal Radiology, 2017, 46(2): 191-199

[30] Xiao Q Li, Hong N Chen, Zhi Yang, et al. Differential diagnostic value of benign and malignant thyriod nodules by real-time shear wave elastography[J]. Journal of Clinical Ultrasound in Medicine, 2016, 18 (4): 233-236

[31] Shih C C, Qian X, Ma T, et al. Quantitative assessment of thin-layer tissue viscoelastic properties using ultrasonic micro-elastography with Lamb wave model [J]. IEEE Transactions on Medical Imaging, 2018, PP(99): 1-1

[32] Tamura N, Nukada T, Kato T, et al. The use of sonoelastography to assess the recovery of stiffness after equine superficial digital flexor tendon injuries: A preliminary prospective longitudinal study of the healing process[J]. Equine Veterinary Journal, 2017, 49(5): 590

[33] Confocal Shear Wave Acoustic Radiation Force Optical Coherence Elastography for Imaging and Quantification of theIn VivoPosterior Eye [J]. IEEE Journal of Selected Topics in Quantum Electronics, 2018, 25(1): 1-7

·重要信息·

《现代生物医学进展》2019 年封面设计说明

此版封面的主体为肿瘤细胞与效应 T 细胞，并特别突出显示了肿瘤细胞表面所表达的免疫抑制受体 PD-L1。众所周知，2018 年诺贝尔生理学或医学奖授予了美国科学家詹姆斯·艾利森和日本科学家庶佑，以表彰他们所发现的抑制免疫负调节的癌症疗法——“免疫检查点疗法”，而 PD-1/PD-L1 通路正是该疗法所针对的一条十分重要的免疫抑制性信号通路。近年来，新兴的肿瘤免疫疗法蓬勃发展，PD-1/PD-L1 抑制剂作为其重要代表，一经问世就朝着靶向治疗，精准治疗的方向不断前行，为癌症治疗开创了全新的免疫治疗思路。

2019 年度杂志封面选择新型的肿瘤免疫疗法为主题，紧跟诺贝尔获奖热点，所表现内容辨识度高，符合《现代生物医学进展》的办刊主旨和特色。